Experimental observation of moving intrinsic localized modes in germanium

Juan F. R. Archilla, Sergio M.M. Coelho, F. Danie Auret, Cloud Nyamhere, Vladimir I. Dubinko, and Vladimir Hizhnyakov

Abstract Deep level transient spectroscopy shows that defects created by alpha irradiation of germanium are annealed by low energy plasma ions up to a depth of several thousand lattice units. The plasma ions have energies of 2-8 eV and therefore can deliver energies of the order of a few eV to the germanium atoms. The most abundant defect is identified as the E-center, a complex of the dopant antimony and a vacancy with and annealing energy of 1.3 eV as determined by our measurements. The inductively coupled plasma has a very low density and a very low flux of ions. This implies that the ion impacts are almost isolated both in time and at the surface of the semiconductor. We conclude that energy of the order of an eV is able to travel a large distance in germanium in a localized way and is delivered to the defects effectively. The most likely candidates are vibrational nonlinear wave packets known as intrinsic localized modes, which exist for a limited range of energies. This property is coherent with the fact that more energetic ions are less efficient at producing the annealing effect.

Key words: Germanium, ILM, discrete breathers, quodons, defects, DLTS

J.F.R. Archilla
Group of Nonlinear Physics, Universidad de Sevilla, ETSI Informática, Avda. Reina Mercedes s/n 41011, Seville, Spain, e-mail: `archilla@us.es`

S.M.M. Coelho and F.D. Auret
Department of Physics, University of Pretoria, Lynnwood Road, Pretoria 0002, South Africa,

C. Nyamhere
Physics Department, Midlands State University, P. Bag 9055, Gweru, Zimbabwe

V.I. Dubinko
NSC Kharkov Institute of Physics and Technology, Akademicheskya Str. 1, Kharkov 61108, Ukraine

V. Hizhnyakov
Institute of Physics, University of Tartu, Ravila 14c, 50411 Tartu, Estonia

1 Introduction

In science like in many other aspects of human activity, there are often fortunate coincidences that orientate research in unexpected directions. In 2012 there was an international workshop in Pretoria, South Africa, called NEMI 2012 [1]. Several theoreticians and nonlinear physicists attended, among them there were two of the authors. Several talks were intended for non specialist in order that physics students could be able to understand them. One of the subjects was nonlinear localized excitations that travel along a periodic media without losing energy and keeping their shape. They are called intrinsic localized modes (ILMS) or discrete breathers (DBs). The first name emphasizes the internal character of the phenomenon and reminds us of the linear vibration modes or phonons. The latter name comes from the observation of the internal vibration they experience that can be compared with the breathing of a living being. They were first obtained as an exact solution for the continuous sine-gordon equation [26]. Simulations using molecular dynamics are able to reproduce them in several solids with energies of the order of a few tenths or a few units of an eV.

Among the attendants was a PhD student, part of a research group of the University of Pretoria working on defects in semiconductors, particularly in germanium. They have obtained unexpected results while treating Ge with low energy (2-8 eV) plasma ions. Those energies are known as subthreshold because the threshold energy to produce displacements of atoms in germanium is between 11.5 for the $\langle 111 \rangle$ direction and 19.5 eV for the $\langle 100 \rangle$ direction [12]. However, they had observed that something was penetrating at least two μm inside the germanium wafer and was able to anneal several defects, in particular, the most abundant one, the E-center. The energy for annealing an E-center is about 1.3 eV, according to our measurements and theoretical calculations [23]. On the other hand the maximum energy that an Ar ion of 4 eV can transmit to a Ge atom is 3.6 eV, therefore the energies were precisely what was expected for ILMs. A line of collaboration was started that joined nonlinear theory, computer simulations, plasma physics and semiconductor physics that eventually confirmed ILMs as the most likely cause of the annealing [1] and also suggested them as the explanation for other long-distance effects such as the modification of defects by electron beam deposition, where the energy transmitted was below 1.3 eV [5]. In this workd we will try to give an explanation of the different branches of the physics involved and to analyze the reasoning that leads to the ILM explanation and the consequences both for semiconductor physics and nonlinear physics.

2 Germanium

The diamond structure of germanium is well known, each atom has covalent bonds with the four nearest neighbours at the vertices of a tetrahedron as shown if Fig. 1. Normally a conventional cubic unit cell comprised of 8 atoms is used. The diamond structure can be seen as an fcc lattice with two atoms at points $(0,0,0)$ and at 1/4 of the diagonal [2]. The lattice unit is $a = 5.66$Å for Ge, slightly larger than 5.43Å for Si and even larger than 3.57Å for C diamond. The diamond structure is not the best for moving ILMs because there is no chain of nearest neighbours forming a straight line. This is a reason for which, although stationary ILMs have been constructed with molecular dynamics [24], the attempts to construct moving ILMs have failed so far. Several lines of research seem promising, one option is to construct ILMs in the next neighbour directions such as $\langle 100 \rangle$ where there is a straight line of atoms. Other is to study polarizations as the ones observed for ballistic phonons in germanium or silicon [13, 19] which can travel distances of 160 nm. It seems also possible that ILMs can be nonlinear perturbations of linear optical modes with high energy, high velocity, short wavelength and low dispersion, such as at the middle of the Brillouin zone for optical branches.

The number of Ge atoms per unit volume can be obtained as $n_{Ge} = 8/a^3 = 4.42 \times 10^{22}$ cm^3. Other properties of interest are atomic number 32, atomic mass $M = 72.61$ amu, density $\rho = 5.323$ g/cm^3, sound velocity $c_s = 5400$ m/s, Debye temperature $T_D = 360$ K, Einstein temperature $T_E = 288$ K, covalent radius 1.22 Å, atomic radius 1.52 Å, melting point 1210.55 K, 1st ionization energy 7.899 eV and specific heat 0.32 J/gK at 300 K.

Fig. 1 Diamond structure of germanium. Each atom is bonded with four nearest neighbours at the vertices of a tetrahedron. The conventional cubic unit cell usually used is also shown. It includes 8 atoms and can be seen as an fcc lattice with two atoms at 0 and at 1/4 of the diagonal. The primitive cell has these two atoms as a basis and the primitive vectors have their origin at 0 and end at the center of each adjacent face
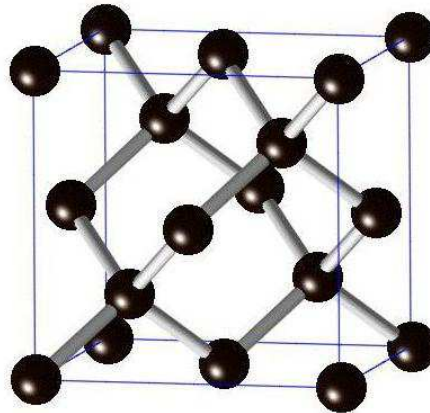
3 Phonons in Ge

The objective of this subsection is to review the well known concepts of lattice dynamics and to see how they apply to Ge and to justify subsequent calculations. Phonons are the usual means for energy transport in a crystal and the responsible party for thermal annealing of defects. With this review we want to demonstrate that they cannot be th responsible for the annealing of the E-center defect during Ar plasma bombardment. We will frequently use general concepts of lattice dynamics and the reader can consult any textbook, for example Refs. [2, 7].

In classical mechanics for a crystal with n_{at} per unit volume, there are $3n_{at}$ degrees of freedom. In the harmonic approximation the substitution of $u_{k,\omega} = \mathbf{A}\exp(\mathbf{i}\mathbf{k}\cdot\mathbf{r} - \omega t)$ in the equation of movement leads to $3n_{at}$ different linear modes of frequency ω, wave number $\mathbf{k}$, phase velocity $c = \omega/k$ and polarization $\mathbf{A}$. They are organized in branches $\omega = \omega(k)$, three of them are acoustic, that is ω vanishes linearly with k in the long wavelength limit. If the crystal has a basis of p atoms or ions in each primitive cell, there are also $3(p-1)$ optical branches, that are bounded from below. In Ge with two Ge atoms in the unit cell, there are three optical branches. Each branch has $n_{Ge}/2$ modes. In the classical description, each mode can have any energy E with a probability at temperature T given by Maxwell-Boltzmann equation $P(E) = \exp(-E/k_BT)/k_BT$, which leads to an average energy k_BT that is identical for each mode. Therefore, it is trivial to obtain the energy per unit volume
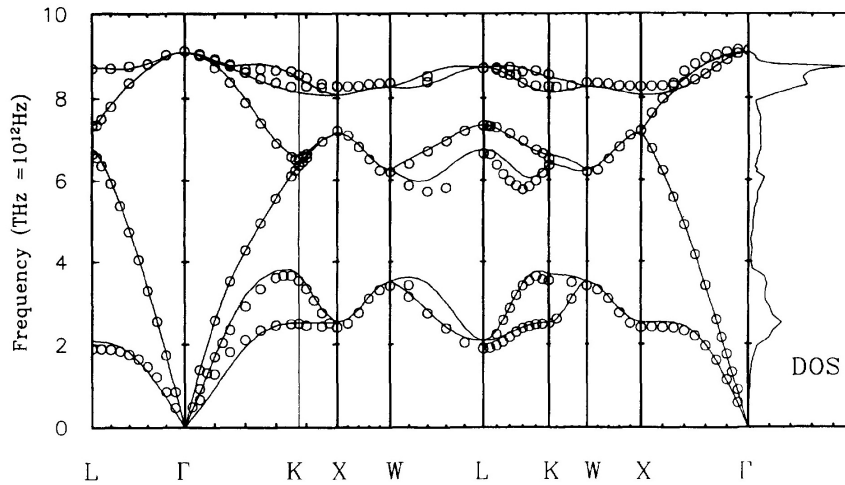

Fig. 2 Phonon dispersion and density of states for Ge. Experimental values are shown as circles and theoretical calculation are shown as solid lines. Modes about the center of some optical bands with high frequency, large group velocity, short wavelength and low dispersion may convert into ILMs when the amplitude enters the nonlinear range. Reproduced with permission from: Wei, S., Chou, M.Y.: Phonon dispersion of silicon and germanium from first principles calculations. Phys. Rev. B **50**, 2221 (1994). Copyright (1994) by American Physical Society

Fig. 3 Primitive Wigner-Seitz reciprocal cell for an fcc lattice such as Ge, showing the directions in *k*-space and points that appear in the spectrum shown in Fig.2. The point Γ corresponds to wave number $k = 0$, where the three acoustical bands originate. The Wigner-Seitz cell is the region of *k*-space that is closer to (0,0,0) than to any other point of the lattice. Modes with wave vectors about the middle of Γ-L, Γ-K and Γ-X may convert into ILMs when their amplitude increases. Axes are the same as in Fig. 1
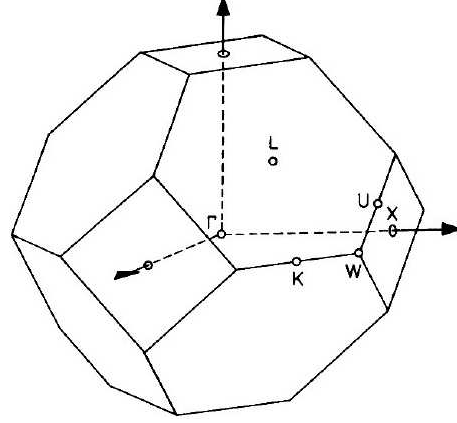
$u = 3k_B T n_{\text{Ge}}$ and the specific heat at constant volume $c_V = \partial u / \partial T = 3k_B n_{\text{at}}$, a result known as the Dulong-Petit law. This result is approximate at room temperatures and above but fails spectacularly at lower temperatures, which led to the quantum description of the harmonic crystal. The classical description of the linear modes of the crystal remains valid but the statistics are quite different.

In quantum mechanics a linear oscillator with frequency ω can only have energies given by $E_n = \frac{1}{2}\hbar\omega + n\hbar\omega$, where n is the excitation or occupation number. As the ground state energy $\frac{1}{2}\hbar\omega$ cannot be lost we will usually suppress it and use

$$E_n = nE, \quad \text{with} \quad E = \hbar\omega, \tag{1}$$

where $E = \hbar\omega$ is the quantum of energy, also called the energy level.

At a given temperature T, the average values $\langle n \rangle$ and $\langle E_n \rangle$ can be obtained with Bose-Einstein statistics. They are

$$\langle n \rangle = \frac{1}{e^{E/k_b T} - 1} \quad , \quad \langle E_n \rangle = \langle n \rangle E = \frac{E}{e^{E/k_b T} - 1}, \tag{2}$$

where $k_B = 8.617 \times 10^{-5}\,\text{eV/K}$ is the Boltzmann constant.

In a solid with $3n_{\text{at}}$ degrees of freedom and therefore the same number of linear modes, each one is equivalent to a linear oscillator with a given frequency ω. It is usual to describe them as phonons or quasi-particles and to use the expression n phonons of a particular type with energy $E = \hbar\omega$ instead of a linear mode or state with frequency ω and excitation number n. We will also follow this convention although in some instances it may be more convenient to revert to the original terminology.

As the number of frequencies is very large and they are very close, ω and $E = \hbar\omega$ are considered as quasi-continuous variables. Most energy levels are degenerate, i.e.,
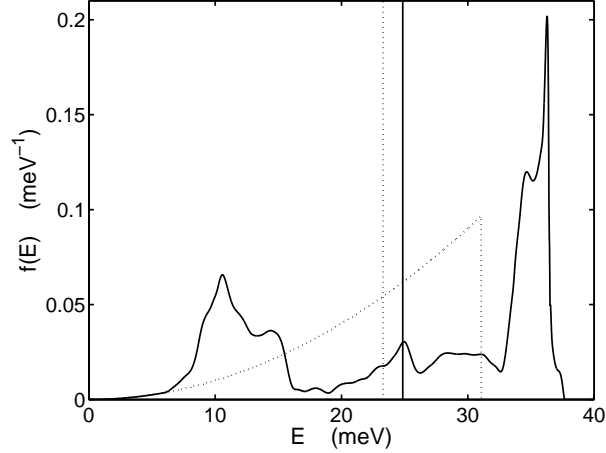
Fig. 4 Comparison with the number function or normalized density of states for germanium: obtained from Fig. 2 and Ref. [25] (—); Einstein model with $T_E = 288$ (vertical —) ; Debye model with $T_D = 360$ ($\cdots$). The mean mode energy is for the first two $E_{\text{ph}} = k_B T_E \simeq 25$ meV. The Debye model by definition has a maximum energy $K_B T_D = 31$ meV with average energy 23.3 meV equivalent to 270 K (vertical $\cdots$) smaller than the Einstein's one. The acoustic and optical bands can be seen although they overlap

there is more than one mode with that energy, and in the quasi-continuous description there are very many in an interval $[E, E + \mathrm{d}E]$.

A variable density of states (DOS) $g(E)$ is introduced, also some times called the density of levels. It is defined such as $g(E)\mathrm{d}E$ is the number of linear modes or quantum phonon states per unit volume with energies between E and $E + \mathrm{d}E$. For a discrete system the phonon spectrum is always bounded from above, that is, there is a maximum frequency and energy ω_M and $E_M = \hbar \omega_M$, therefore

$$\int_0^{E_M} g(E)\mathrm{d}E = 3n_{\text{at}}. \tag{3}$$

A rough estimate of the maximum value of energy level for the acoustic modes can be obtained using the fact that the minimum value of the wavelength is twice the lattice unit of the primitive cell d_a, then $E_{\text{M,ac}} \simeq \hbar \omega_{M,ac} = \hbar c 2\pi / 2 d_a$, with c the speed for the mode. For Ge, $d_a = a/\sqrt{2} = 4.00$ Å and using $c_s = 5400$ m/s, we obtain $E_{\text{M,ac}} = 28$ meV and $f_{\text{M,ac}} = 6.7$ THz similar at the observed values in Figs. 2 and 3. However, such a simple estimate for the optical modes is not possible because the phase velocity tends to infinity when $k \to 0$.

Generally speaking there is no minimum frequency or energy as explained above, however, when considering only a part of the system, it can be described as subjected to an external potential representing the interaction with the rest of the crystal. In this case the phonon spectrum becomes optical, i.e., bounded from below.

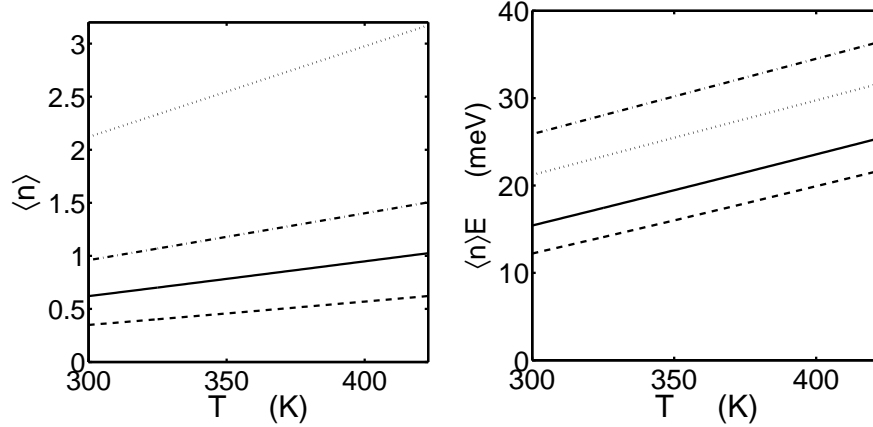The energy of the solid per unit volume is given by

Fig. 5 (Left): Average number of phonons with respect to temperature between room temperature $T_R = 300\,$K and E-center annealing temperature $T_A = 423\,$K. From bottom to top: optical phonons with $E_{op} = 35\,$meV; Einstein phonons with $E_E = 24.9\,$meV; average number of phonons with Ge DOS; acoustic phonons with $E_{ac} = 10$. (Right): Average energy for different phonons, from bottom to top: optical phonons with $E_{op} = 35\,$meV; Einstein phonons with $E_E = 24.9\,$meV ($T_E = 288\,$K) indistinguishable from the one obtained with Ge DOS; acoustic phonons with $E_{ac} = 10\,$meV and average classical energy $k_B T$. It can be seen that the acoustic modes have more phonons and more energy than the optical ones and at room temperature and above a quantum description is necessary

$$u_E = \int_0^{E_T} \langle n(E)\rangle E\, g(E)\mathrm{d}E = \int_0^{E_T} \frac{E}{e^{E/k_b T} - 1} g(E)\mathrm{d}E\,. \tag{4}$$

We will also use the number density or normalized density of states $f(E) = g(E)/3n_{\text{Ge}}$, with the property that as $f(E)\mathrm{d}E$ is the fraction of modes with energies between E and $E + \mathrm{d}E$ and therefore the normalization condition and average phonon energy E_{ph} are given by

$$\int_0^{E_T} f(E)\mathrm{d}E = 1 \quad , \quad E_{\text{ph}} = \int_0^{E_T} E f(E)\mathrm{d}E\,. \tag{5}$$

There are two approximations frequently used for the density of states: the Debye and the Einstein models. In the Debye model, all phonon modes are substituted by three acoustic branches with dispersion relation $\omega = ck$, with the same c, which is an average velocity. These acoustic branches lead to a density of modes or states per unit volume $g_D(E) = 3/(2\pi^2\hbar^3)c^3 E^2$ [2]. Then, $f_D(E) = g(E)/n_{\text{at}} = \alpha_D E^2$, with the constant α_D depending on the particular solid through c and n_{at}. The energy has a cutoff value E_D such that the condition of normalization $\int_0^{E_D} f_D(E)\mathrm{d}E = 1$ is fulfilled. Therefore, $\alpha_D E_D^3/3 = 1$. The values E_D and $T_D = E_D/k_B$ are known as the Debye energy and temperature, respectively. Therefore there is only one unknown, either c or T_D, either of which cannot be measured as they do not correspond to real magnitudes. What is done is to choose T_D such that the specific heat $c_v(T)$

fits the measurements. For Ge, a value of $T_D = 360\,K$ or $E_D = k_B T_D = 31.1\,meV$ is usually given, which corresponds to $c = 3420\,m/s$. This velocity is not a real quantity but coherently it is approximately the mean of the velocities of the two transversal modes, $\simeq 2500\,m/s$, and the longitudinal one, $5400\,m/s$ [15]. The Debye dispersion relation works, of course, better for the acoustic branches and small wave vectors.

The Einstein model supposes that there are $3n_{\mathrm{Ge}}$ modes with the same frequency ω_E, being $E_E = \hbar\omega_E$ and $T_E = E_E/k_B$, the Einstein energy and temperature, respectively. The value of T_E is chosen so as to fit the specific heat of the solid, being E_E an average energy of the phonons in the crystal. For germanium its value is $T_E = 288\,K$ and will be used in this work. In this model the mean energy per unit volume at temperature T in germanium is simply

$$u_E = \frac{3n_{\mathrm{Ge}}}{\mathrm{e}^{E_E/k_B T} - 1} \tag{6}$$

The actual phonon dispersion relation and the density of states have been obtained and checked with experimental ones in Ref. [25]. Both magnitudes are shown in Fig. 2. The normalized density of states $f(E)$ can be obtained from it but as the resolution is poor for low energies we have substituted that part by the Debye one. The Ge density of states is shown in Fig. 3 together with the corresponding one for
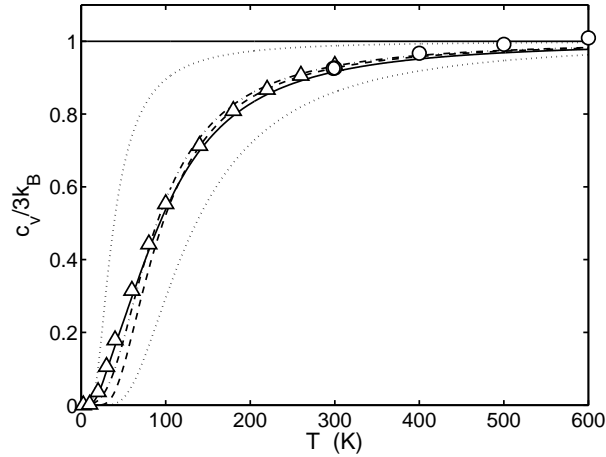

Fig. 6 Comparison of the experimental specific heat per degree of freedom: (–) using germanium density of states [25]; (- -) the Einstein model with $T_E = 288$; ($- \cdot -$) the Debye model with $T_D = 360$; (○) and (Δ) experimental values from Refs. [3,17], respectively. The horizontal line corresponds to the classical Dulong-Petit law. The Einstein and the Debye model are slightly better at intermediate temperatures, because they have been fitted for that. At high temperatures the experimental c_v becomes larger because actual frequencies also increase with temperature. The two separated dotted curves correspond to two Einstein models with energies $E_{\mathrm{ac}} = 10$ and $E_{\mathrm{op}} = 35\,meV$, the upper and lower curves, respectively. These values are representative of the acoustic and optical branches

the Debye and Einstein model for comparison. For $g(E)$ two concentrations of states appear near the top and near the bottom of the spectrum, with a drastic simplification we can describe them as an optical band around $E_{\text{op}} = 35\,\text{meV}$ and an acoustic one around $E_{\text{ac}} = 10\,\text{meV}$. The mean phonon energy $\int_0^{E_T} f(E) E \, dE$ is approximately equal to the Einstein energy.

Figure 3 represents the number of phonons and the average energies as a function of temperature for acoustic phonons, optical phonons, Einstein phonons, and average values obtained with the density of states $g(E)$. It can be seen that the classical statistics is not valid at the temperatures of interest in this work and that there are significant differences between optical and acoustic phonons. The energy in the acoustic modes is larger than in the optical ones in spite of having less energy but with more phonons. It can also be seen that the average number of phonons $\langle n \rangle$ is smaller or closer to one which indicates that the classical description is not good at room temperatures and above.

Figure 3 represents the specific heat at constant volume obtained from these models. There is no significant difference at the temperatures of interest in this work between room temperature $T_R = 300\,\text{K}$ and the annealing temperature of the E-center $T_A = 423\,\text{K}$. This justifies the use of the Einstein density of states as a good approximation for calculations. The specific heats for two Einstein models with E_{ac} and E_{op} are also represented for comparison.

4 Defects and their detection with DLTS

Point defects in the structure or the type of atoms of the semiconductor can appear with some probability due to the temperature but they can also be created by radiation. In the experiments described in this work most of the defects are created by $5\,\text{MeV}$ alpha radiation [14, 21] produced in the decay of the americium isotope ^{241}Am. A Ge sample with dimensions $3 \times 5 \times 0.6\,\text{mm}$ is brought into contact with americium foil for 30 minutes.

Defects can be of many types, some simple examples are shown in Fig. 7, such as a vacancy, a substitutional atom, a self-interstitial, a foreign interstitial, a Frenkel pair that is, a combination of a vacancy and a self-interstitial and an E-center, which is a combination of a dopant substitutional atom and a vacancy. The germanium sample used in this work is doped with antimony (Sb), with a dopant concentration $n_{\text{Sb}} = 1.3 \times 10^{15}\,\text{cm}^{-3}$. Dopant atoms as Sb atoms occupy substitutional positions but are not considered defects as they are an essential part of the semiconductor electrical properties. The main defect appearing after α irradiation is the E-center already described. There are many others types such as vacancy complexes like the di-vacancy (V-V), the tri-vacancy (V_3), the tetra-vacancy (V_4) and combinations of interstitials as di or tri-interstitials (I_2, I_3). Also, hydrogen (H), due to its small size is able to penetrate almost everywhere and can combine with other defects forming complexes such as VH_n, where n is an integer with values from $1 - 4$. A variant of the E-center is the A-center, a complex of an oxygen interstitial and a vacancy.
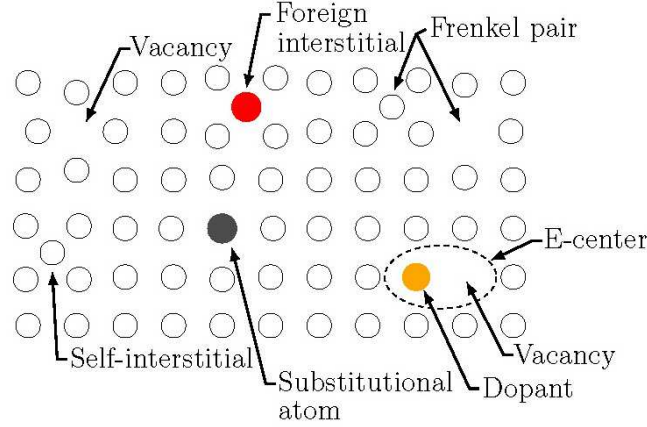
Fig. 7 Examples of some point defects in a crystal. The E-center studied in this work is a complex of a vacancy and a substitutional dopant Sb

Defects can experience many processes like diffusion, interaction between them, modification, annealing and others. Generally speaking all these processes are enhanced by temperature and the rate at which the process takes place depends in an Arrhenius form on a quantity known as the enthalpy for the process or sometimes referred to as the activation energy or barrier energy for the process. That is

$$\kappa \propto e^{-\Delta H / k_B T} . \tag{7}$$

The semiconductor Ge has a band gap of $E_g = 0.67$ eV. Some defects introduce electrical levels inside the band of a semiconductor, as for example in Sb-doped Ge, Sb introduce levels very close to the conduction band. When they are within the band gap and more than 0.1 eV from the conduction or the valence bands they are considered *deep*. Usually they are called electron *traps* when they introduce an electron level and hole traps when they introduce a hole level, respectively. We will write only about electron traps for simplicity, because the treatment of holes is very similar, and because the main defect we are interested in, the E-center, is an electron trap. The E-center is located at $E_T = 0.38$ eV below the conduction band. The same defect has also been reported as $E_T = 0.37$.

When an electron is in a trap level it has a mean time of permanence τ_n and its inverse $e_n = 1/\tau_n$ is the probability of emission per unit time. This magnitude and its dependence on temperature are key to defect detection as it is the actual magnitude measured in DLTS [16, 22]. This dependence can be easily deduced.

Suppose that there are N_T traps per unit volume, the probability for an electron occupying the trap level of energy E_t (not E_T which is $E_T = E_c - E_t$) is given by the Fermi-Dirac distribution

$$f_t = \frac{1}{e^{(E_t - E_F)/K_B T} + 1} , \tag{8}$$

where E_F, the Fermi energy is located near the middle of the phonon band.

The probability that a moving electron is captured by a trap is given by $c_n = \sigma_{app} v_{th} N_T (1 - f_t) n$, where σ_{app} is the capture cross section of an electron for the trap, $v_t h$ is the thermal velocity of the electrons, N_T the trap concentration, $(1 - f_t)$ the probability of the trap being empty and n the number of electrons per unit volume. The latter quantity can be obtained as $n = N_c \exp(-(E_c - E_F)/k_B T)$, where E_c is the bottom energy of the conduction band, m_e^* being the effective mass of an electron and $N_c = 2 (2\pi m_e^* k_B T / h^2)^{3/2}$ is the effective density of states in the conduction band [2]. The thermal velocity can also be obtained as $v_{th} = (2E_{th}/m_e^*)^{1/2}$, with $E_{th} = 3/2 k_B T$.

The trap emission rate r_n is given by $r_n = N_T f_t e_n$, that is, the concentration of traps multiplied by the probability of being occupied and the probability of emission per unit time for a trap. At thermal equilibrium $c_n = r_n$ and e_n can be isolated as

$$e_n = \sigma_{app} N_c v_{th} \exp(-E_T/k_B T), \tag{9}$$

with $E_T = E_c - E_t$, that is, the distance of the trap level to the conduction band.

It is easy to check that the pre-exponential factor is proportional to T^2 as the effective mass is approximately constant at the bottom of the conduction band where most of the occupied states are.

Some authors discuss the interpretation of this expression of the emission rate [6] as a function of the capture parameters, however σ_{app} and E_T are considered the defect signature and used worldwide. Independently of the meaning σ_{app} has the right dependence on the temperature and should simply considered simply as a parameter of the defect.

The technique known as DLTS, deep level transient spectroscopy, uses a pn junction or a metal-semiconductor junction known as a Schottky diode. A voltage pulse is sent through the junction in reverse bias, so as to flood all the traps with electrons, which after the pulse start to emit electrons towards the conduction band at a rate given by Eq. (9). The capacitance of the junction depends on the charge accumulated in the traps and therefore changes with time as the traps become depleted. It is measured at two different times t_1 and t_2. If C_0 is the capacitance at t_1 and ΔC the change in the capacitance between t_1 and t_2, it can be demonstrated that the relative change in the capacitance $\Delta C/C_0$ has a maximum when the so called rate window equals the emission probability:

$$RW \equiv \frac{\ln(t_1/t_2)}{t_1 - t_2} = e_n. \tag{10}$$

Typical rate windows are $80\,\mathrm{s}^{-1}$ and $200\,\mathrm{s}^{-1}$. Measurements of the DLTS signal $\Delta C/C_0$ are performed while the temperature T is changed. When the RW equals the emission rate of some defect a peak appears in the plot of $\Delta C/C_0$ with respect to T. In this way the different defects appear. At the peak

Fig. 8 DLTS Arrhenius plots of some electron trap defects observed in Ge. The E-center, here marked as $E_{0.38}$ figures among them. Reproduced with permission from: Coelho, S.M.M., Auret, F.D., Janse van Rensburg, P.J., Nel, J.: Electrical characterization of defects introduced in n-Ge during electron beam deposition or exposure. J. Appl. Phys. **114**(17), 173,708 (2013). Copyright (2013) by AIP Publishing LLC
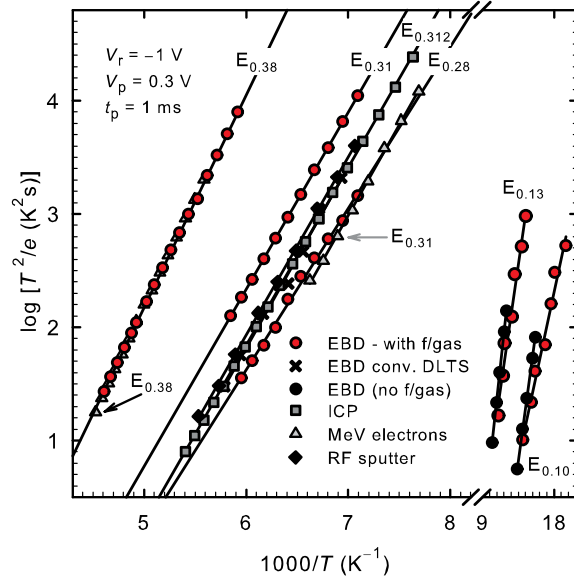
$$N_T = 2 \left(\frac{\Delta C}{C_0} \right)_{\text{peak}} N_D, \tag{11}$$

where N_D is the number of dopants in an n-type semiconductor and N_T is the number of traps corresponding to the peak. Using several RWs, several values of e_n can be obtained for different temperatures, being E_T the slope of the representation $\ln(T^2/e_n)$ with respect to $1/T$. From the same representation the value of σ_{app} can be obtained and therefore the defect is fully characterized. From the height of the peak the concentration of the defect N_T can also be obtained. The value of the reverse bias determines the depth of the measurements and allows for the plotting of the profile of N_T as a function of the depth of the sample. This procedure to characterize the E-center in Ge was performed in Ref. [5] and the Arrhenius plots for several defects can be seen in Fig. 8.

5 Experiment of plasma-induced annealing

The main experiment is done as follows: (a) The Ge wafer is bombarded with 5 MeV alpha particles during 30 minutes and it is left for 24 hours at room temperature for the defects to stabilize as initially there is a fast kinetic [11]; (b) The surface of Ge is divided into two parts *A* and *B*, then a diode is made using resistive evaporation of Au on part *A* and DTLS is performed to measure the defect concentrations, (c) The Ge sample is introduced into an inductively coupled plasma (ICP) with 4 eV Ar ions and pressure of 0.1 mb for half an hour in intervals of 10 minutes to allow for

cooling; (d) DTLS is performed in part *A*, where ICP has been done through Au, (e) A diode is evaporated on part *B*, where ICP has been applied directly on the Ge surface, and then, DTLS is performed there.

The short time of alpha irradiation is done to allow for better DLTS measurements. A concentration of about 10% of N_D, as the was obtained, or less is ideal

The results of the three measurements are presented in Fig. 5. We will concentrate on the most abundant defect, the E-center. (1) The concentration after alpha damage and 24 hours rest is $N_T = 1.07 \times 10^{14}\,\text{cm}^{-3}$; (2) After direct ICP on germanium it is reduced by 30%; (3) If the ICP is applied through the Au contact, the reduction is about 7%, smaller but still significant.

Other details of interest are: (4) The sample heats up to about 40°C in spite of the cooling intervals; (5) If there is no cooling the sample heats up to about 65°C and the decrease in the rate of annealing is dramatic; (6) The defects are annealed up to a depth of 2600 nm inside the Ge sample [1]; (7) If other metals are used for the
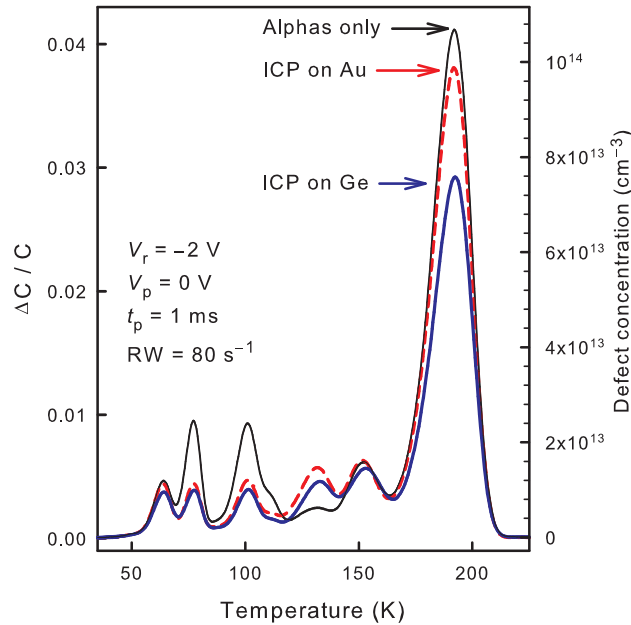

Fig. 9 DTLS spectra showing the experimental results. The defect concentrations on the right axis are only valid for the peaks. The main peaks correspond to the E-center defect. A 30% diminution of the concentration of this defect can be observed after 30 minutes under the action of an inductively coupled plasma (ICP) with 4 eV Ar ions. If the ICP is applied through the Au contact the diminution exists although it is substantially smaller. Reproduced with permission from: Archilla, J.F.R., Coelho, S.M.M., Auret, F.D., Dubinko, V.I., Hizhnyakov, V.: Long range annealing of defects in germanium by low energy plasma ions. Physica D **297**, 56–61 (2015). Copyright (2015) by Elsevier

contact the annealing also takes place as with Au but the effect depends on the metal used; (8) If a plasma of larger energy 8 eV is used the annealing rate increases, but given that a plasma of larger energy also has a larger flux, the effect per Ar ion is much smaller (see below); (9) The temperature to achieve a similar rate of annealing is 150°C as deduced in Sect. 7 and by other authors [18].

There was no measurable concentration of Ar after ICP which discards Ar channelling. Other explanations were considered and discarded in Ref. [1] such as multivacancy production, production of minority charge carriers, production of defects that could diffuse and interact with the E-center and diffusion of H that could passivate the vacancies in the E-center.

6 ILM hypothesis

In this section we analyze the experiment and examine the possibility that Ar ions produce intrinsic localized modes that travel in a localized way with little dispersion through the semiconductor and are able to anneal the defects. The exact nature of these ILMs is not yet known but here it is assumed that they have a vibrational part due to their origin from an Ar ion hit. If they have also some charge or other properties is unknown and not necessary for this hypothesis.

The rate of ion-induced annealing is given by the following equation:

$$\frac{dN_T}{dt} = -\sigma_i \Phi_i N_T \,, \tag{12}$$

where σ_i is an effective cross-section for defect annealing by plasma ions. It is as if imaginary Ar ions would penetrate Ge and anneal a defect but at this stage there is no need of an hypothesis, σ_i is just the probability per unit time and unit flux of Ar ions that a defect is annealed. Integrating the equation above we obtain:

$$N_T(t) = N_T(0)e^{-\sigma_i \Phi_i t} \quad \text{or} \quad \sigma_i = -\frac{1}{\Phi_i t} \ln \frac{N_T(t)}{N_T(0)} \tag{13}$$

For the experiment described with pressure $p = 0.1$ mb, that corresponds to 4 eV ions, the flux is $\Phi_i = 5.58 \times 10^{10}$ cm^{-2}s^{-1} [1], $t = 30 \times 60$ s and $N_T(t)/N_T(0) = 0.7$, and $\sigma_i \simeq 35.6$ Å^2 is obtained. This value should be compared with $\sigma_0 = (n_{Ge})^{-2/3} \simeq 8$ Å^2, that is, the average area corresponding to an atom of Ge at the surface of the semiconductor, then $\sigma_i \simeq 4.4\sigma_0$. This result indicates that the process has an enormous efficiency. It has to be considered with caution as also neutrals may be arriving at the semiconductor surface, but it should not change the result by more than one order of magnitude, probably by around a factor of two in the flux.

It is interesting to see what the change in efficiency is when an 8 eV plasma is used. The flux in this case is $\Phi_i(8\,\text{eV}) = 1.35 \times 10^{13}$ cm^{-2}s^{-1} [1] and using only 600 s time the concentration is reduced to 80% of the original. The cross section becomes $\sigma_i(8\,\text{eV}) \simeq 0.26$ Å$^2 \simeq 0.033\sigma_0$. Therefore a larger energy per Ar ion does

not increase the efficiency of the ion-annealing process but reduces it by a factor of $\simeq 140$. This is coherent with our hypothesis that the Ar^+ impacts produce ILMs, because ILMs have a definite range of energies. More energy than what is required will be dispersed into phonons which would interfere with the propagation of the ILMs. It is also interesting to be aware of a few magnitudes to appreciate what could be happening in the semiconductor. Suppose that ILMs travel at a speed of the order of magnitude of the speed of sound in Ge, $c_s = 5400$ m/s, the time needed for an ILM to travel the measured depth $d = 2600$ nm is $\delta t = 0.5$ ns. This means that the area for an Ar^+ hit in δt is a circle with a radius of about 10^6 lattice units, or in other words each impact and travel is completely isolated.

Note also that the traps are almost isolated as $(N_T)^{-1/3} \simeq 2200$ Å or 370 lattice units. Therefore there is no influence between them.

Let us introduce a couple of parameters, γ the efficiency of ILM creation by Ar ions, that is

$$\Phi_{ILM} = \gamma \Phi_i \tag{14}$$

and α the cross section for ILM defect annealing measured in σ_0 units, that is

$$\sigma_{ILM} = \alpha \sigma_0. \tag{15}$$

Therefore

$$\sigma_i = \alpha \gamma \sigma_0 \tag{16}$$

and $\alpha \gamma \simeq 3.6$. The cross section should be larger than σ_0 because the size of an E-center is at least two atoms and due to the complex nature of Ge, ILMs probably have also a complex structure with a few atoms involved perpendicular to the movement of the ILMs. If the interaction takes place at a distance of four atoms then $\alpha \simeq 8^2 \sigma_0$ and $\gamma = 0.06$. The latter result implies that about 20 Ar^+ hits are necessary to produce an ILM. The number of Ar^+ to anneal a defect can also be calculated easily as $\Phi_i t / (0.3 N_T d) \simeq 1.2 \times 10^4$.

In the following section it will be made clear that this rate of annealing cannot be produced only by the increase in temperature. Therefore, although the numbers are approximate and many objections can be made there are a few clear consequences of this analysis: (1) Some entity which we call ILM, and most likely it is a vibrational entity, is able to travel distances of a few micrometers inside Ge in a localized way and without losing much energy (2) There is a high efficiency in the conversion of Ar^+ hits to ILMs; (3) There is a high efficiency for ILMs to anneal or modify defects.

Note that if the annealing barrier is E_A it is neither necessary for an ILM to have nor to deliver E_T to anneal the defect. The change of the barrier due to the passing of an ILM nearby brings about a change in the annealing rate which can be very high. See Refs. [4, 8–10].

7 Thermal annealing

In this section we review thermal annealing and apply it to Ge in order to compare the temperature and energy needed to obtain the same rate of thermal annealing as with Ar ions.

Thermal annealing of defects in semiconductors is given by a first order kinetic

$$\frac{dN_T}{dt} = -KN_T \,, \tag{17}$$

where K, known as the reaction rate constant is given by an Arrhenius type law

$$K = Ae^{-E_a/k_B T} \,, \tag{18}$$

where E_a is known as the annealing energy and A as the pre-exponential factor. E_a can be interpreted as the potential barrier which is necessary to surmount in order that the transformation or diffusion process for annealing takes place. The exponential term can be seen as the probability for an accumulation of energy of magnitude E_a. The pre-exponential term A has units of frequency and it is also known as the frequency factor. It is related to the number of attempts per unit time that the system tries to pass the barrier and with the curvature of the energy with respect to the reaction coordinate. A may also depend on the temperature but in a much weaker way than the exponential term. It also depends on the entropy change.

The integration of Eq. (17) leads to the exponential decay $N_T(t) = N(0)\exp(-Kt)$ and comparing the experimental data with $\ln(N(t)) = \ln(N(0)) - Kt$ it is possible to obtain K. Several data for E-center annealing have been published [11, 18]. Here we will use the results obtained by some of the authors according to the procedure described in Ref. [20] and using the same dopant and defect concentration as in this work. Figure 7(a) shows the exponential decay at $165°$C and Figure 7(b) represents $\ln(N_T)$ with respect to time for three temperatures. The approximate linear dependence can be seen. From the slopes, three values of the reaction rate constant are obtained and in Fig. 7(c) $\ln(K)$ is represented with respect to $1000/T$ and the linear dependence can be observed. Comparing with $\ln(K) = \ln(A) - E_a/k_B T$ the values $A = 5.5 \times 10^{11}\,\text{s}^{-1}$ and $E_a = 1.3\,\text{eV}$ are obtained. These numbers should be treated with caution as the experimental procedure is very sensitive to the details of the experimental technique. The sample has to be cooled and reheated to measure the defect concentration.

8 Comparison of thermal and plasma-induced annealing

Comparing the equations for thermal annealing Eq. (17) and ion-induced annealing Eq. (12) we can observe that if both process have the same rate of annealing
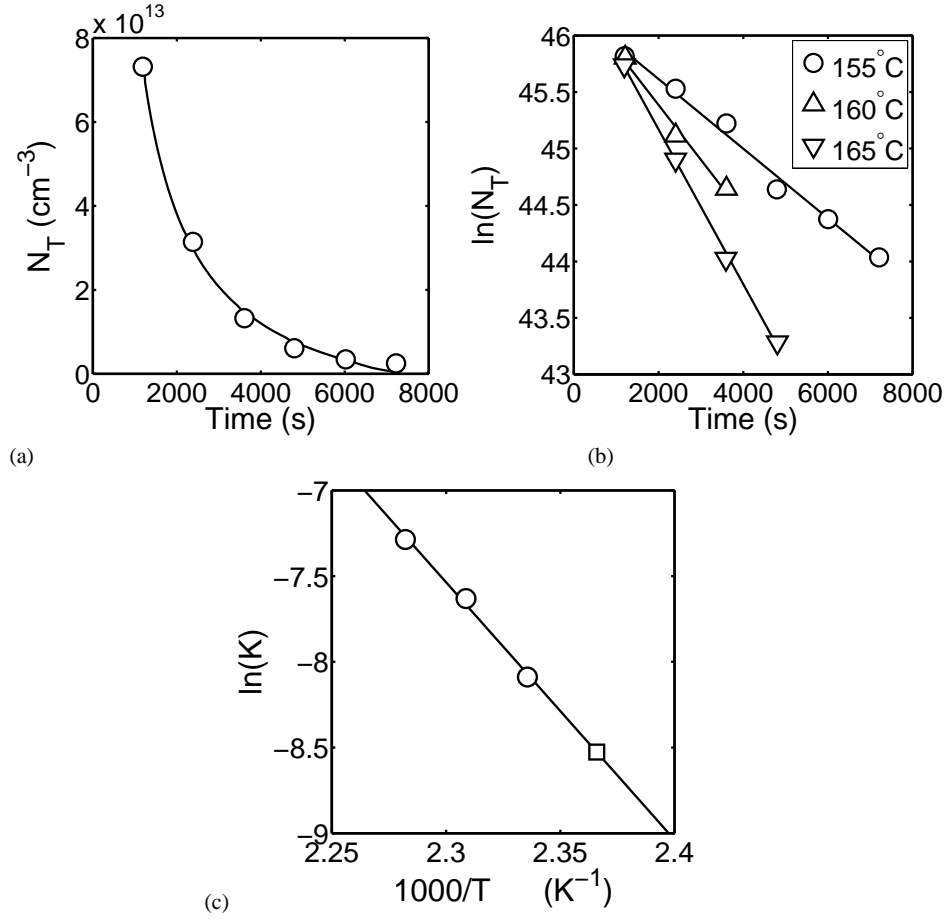
Fig. 10 (a) Defect concentration versus annealing time at $T = 165°C$. (b) Semi-log plot of defect concentration versus annealing time at temperatures 155°C, 160°C and 165°C from which the annealing rate constant, K, is calculated. (c) The Arrhenius plot from which $E_A = 1.3\,eV$, $A = 0.55\,THz$ and $T_A = 423\,K$ are obtained. Lines are fitted curves, circles and triangles are experimental values, the square in (c) corresponds to a thermal annealing rate equal to ion-induced annealing. Details of the experimental procedure used can be read in Ref. [20]

$$K = \sigma_i \Phi_i \quad \text{or} \quad Ae^{-E_a/k_bT} = \sigma_i \Phi_i. \tag{19}$$

From this equation, the value of $T_A = 423\,K$ is obtained.

The thermal energy at T_A per unit volume using Ge density of states $g(E)$ from Sect. 3 is given by

$$u_{\text{ph}} = \int_0^{Em} \langle n \rangle E g(E) dE. \tag{20}$$

Note that the use of the Einstein model with $T_E = 288$ K leads to very similar results. The increment in energy from room temperature $T_R = 300$ K to $T_A = 423$ K is given by

$$\Delta u_{\mathrm{ph}} = u_{\mathrm{ph}}(T_A) - u_{\mathrm{ph}}(T_R) \simeq 2.9\,\mathrm{KJ/mol} \simeq 30.1\,\mathrm{meV/atom}. \tag{21}$$

The energy per unit volume of energy in ILMs is given by

$$u_{\mathrm{ILM}} = \rho_{\mathrm{ILM}} E_{\mathrm{ILM}}, \tag{22}$$

where ρ_{ILM} is the density per unit volume of ILMs and E_{ILM} is the mean ILM energy. Both quantities are unknown but we can estimate both. The maximum flux of ILMs is the flux of ions Φ_i and the maximum energy is the energy that a 4 eV Ar ion can deliver to a Ge atom, 3.6 eV. Let us suppose $E_{\mathrm{ILM}} \simeq 3$ eV and $\Phi_{\mathrm{ILM}} \simeq \Phi_i$. The velocity of ILMs should be of the order of magnitude of the d velocity of sound, $v_{\mathrm{ILM}} \simeq c_s = 5400$ m/s. Then $\rho_{\mathrm{ILM}} \simeq \Phi_{\mathrm{ILM}}/v_{\mathrm{ILM}} \simeq 10^5\,\mathrm{cm}^{-3}$ and the ILM energy per Ge atom is

$$\frac{u_{\mathrm{ILM}}}{n_{\mathrm{Ge}}} = \frac{\Phi_{\mathrm{ILM}} \mathrm{ILM} E_{\mathrm{ILM}}}{v_{\mathrm{ILM}}\, n_{\mathrm{Ge}}} \simeq 7 \times 10^{-15}\,\mathrm{meV/atom}. \tag{23}$$

This value is so small because there is only an ILM for every 4×10^{17} Ge atoms. Therefore the ratio $u_{\mathrm{ILM}}/\Delta u_{\mathrm{ph}} \simeq 10^{-16}$, which proves that an enormously larger amount of energy in phonons is needed in order to produce the same annealing effect than the Ar ions produced. Changes in the ILM energy, their speed, the number of them created by neutrals in the plasma and other factors cannot change their energy density by a factor of 10^{16}.

9 Summary

In this work we have described an experiment in which a low energy, low flux Ar plasma anneals defects in Sb-doped Ge up to a significant depth below the surface. The hypothesis advanced in Ref. [1] and continued here is that Ar ions produce some kind of travelling localized excitation with great efficiency. We call these entities intrinsic localized modes or ILMs because their energy and other properties indicates that their energy is vibrational, although this is by no means demonstrated. Some space has been dedicated to phonons in germanium in order to have a clear picture of them and their energies and so doing clarify that they cannot be responsible for the annealing effect, because the ILM energy density is much smaller than the phonon density which produces the same annealing rate. Also we think that the study of the dispersion relation can bring home ideas about how to construct ILMs in Ge, which will be the confirmation of the present hypothesis but seems to be a daunting challenge.

The numbers are approximate, many hypotheses and estimations that have been advanced may be incorrect, however none of these problems can change the fact of the observation of long-range annealing in germanium produced by Ar plasma and that ILMs are the most promising cause.

Acknowledgments

References

1. Archilla, J.F.R., Coelho, S.M.M., Auret, F.D., Dubinko, V.I., Hizhnyakov, V.: Long range annealing of defects in germanium by low energy plasma ions. Physica D **297**, 56–61 (2015)
2. Ashcroft, N.W., Mermin, N.D.: Solid State physics. Saunders College Publishing, Philadelphia (1976)
3. Berger, L.I.: Semiconductor Materials. CRC Press, London, UK (1996)
4. Coelho, S.M.M., Archilla, J.F.R., Auret, F.D., Nel, J.M.: The origin of defects induced in ultra-pure germanium by electron beam deposition. In: J.F.R. Archilla, N. Jiménez, V.J. Sánchez-Morcillo, L.M. García-Raffi (eds.) Quodons in mica: nonlinear localized travelling excitations in crystals. Springer (2015). To appear
5. Coelho, S.M.M., Auret, F.D., Janse van Rensburg, P.J., Nel, J.: Electrical characterization of defects introduced in n-Ge during electron beam deposition or exposure. J. Appl. Phys. **114**(17), 173,708 (2013)
6. Dimitrijev, S.: Irreversible event-based model for thermal emission of electrons from isolated traps. J. Appl. Phys. **105**, 103,706 (2009)
7. Dove, M.T.: Introduction to lattice dynamics. Cambridge University Press, Cambridge, UK (2005)
8. Dubinko, V.I., Archilla, J.F.R., Dmitriev, S.V., Hizhnyakov, V.: Rate theory of acceleration of defect annealing driven by discrete breathers. In: J.F.R. Archilla, N. Jiménez, V.J. Sánchez-Morcillo, L.M. García-Raffi (eds.) Quodons in mica: nonlinear localized travelling excitations in crystals. Springer (2015). To appear
9. Dubinko, V.I., Dubinko, A.V.: Modification of reaction rates under irradiation of crystalline solids: contribution from intrinsic localized modes. Nucl. Instrum. Meth. B **303**, 133–135 (2013)
10. Dubinko, V.I., Selyshchev, P.A., Archilla, J.F.R.: Reaction-rate theory with account of the crystal anharmonicity. Phys. Rev. E **83**, 041,124 (2011)
11. Fage-Pedersen, J., Larsen, A.N.: Irradiation-induced defects in Ge studied by transient spectroscopies. Phys. Rev. B **62**, 10,116 (2000)
12. Holmström, E., Nordlund, K., Kuronen, A.: Threshold defect production in germanium determined by density functional theory molecular dynamics simulations. Phys. Scr. **81**, 035,601 (2010)
13. Karamitaheri, H., Neophytou, N., Kosina, H.: Ballistic phonon transport in ultra-thin silicon layers: Effects of confinement and orientation. J. Appl. Phys. **113**(20), 204,305 (2013)
14. Kolkovsky, V., Petersen, M.C., Larsen, A.N.: Alpha-particle irradiation-induced defects in n-type germanium. Appl. Phys. Lett. **90**(11), 112,110 (2007)
15. Lacroix, D., Joulain, K., Lemonnier, D.: Monte carlo transient phonon transport in silicon and germanium at nanoscales. Phys. Rev. B **72**, 064,305 (2005)
16. Lang, D.V.: Deep-level transient spectroscopy: A new method to characterize traps in semiconductors. J. Appl. Phys. **45**(7), 3023–3032 (1974)
17. Lide, D.R. (ed.): Handbook of Chemistry and Physics, 90th edn. CRC Press, Boca Raton, Florida, USA (2010)

18. Markevich, V.P., Peakera, A.R., Litvinov, V.V., Emtsev, V.V., Murin, L.I.: Electronic properties of antimony-vacancy complex in Ge crystals. J. Appl. Phys. **95**, 4078 (2004)

19. Northrop, G.A., Wolfe, J.P.: Ballistic phonon imaging in germanium. Phys. Rev. B **22**, 6196–6212 (1980)

20. Nyamhere, C.: Characterization of process and radiation induced defects in Si and Ge using conventional deep level transient spectroscopy (DLTS) and laplace-DLTS. Ph.D. thesis, University of Pretoria (2009). URL `http://upetd.up.ac.za/thesis/available/etd-02022010-134937/`. Viewed 14-03-2014

21. Roro, K., Janse van Rensburg, P., Auret, F., Coelho, S.M.M.: Effect of alpha-particle irradiation on the electrical properties of n-type Ge. Physica B **404**(22), 4496–4498 (2009)

22. Schroder, D.K.: Semiconductor Material and Device Characterization, 3rd edn. John wiley, New Jersey, USA (2006)

23. Tahini, H., Chroneos, A., Grimes, R.W., Schwingenschlo, Bracht, H.: Diffusion of E centers in germanium predicted using GGA+U approach. Appl. Phys. Lett. **99** (2011)

24. Voulgarakis, N.K., Hadjisavvas, S., Kelires, P.C., Tsironis, G.P.: Computational investigation of intrinsic localization in crystalline Si. Phys. Rev. B **69**, 113,201(1–4) (2004)

25. Wei, S., Chou, M.Y.: Phonon dispersion of silicon and germanium from first principles calculations. Phys. Rev. B **50**, 2221 (1994)

26. Wikipedia: Sine-gordon equation. `http://en.wikipedia.org/wiki/Sine-Gordon_equation` (2015). Accessed April 6, 2015